Available online at www.sciencedirect.com
ScienceDirect
Proceedings of the Combustion Institute 31 (2007) 841–849
Proceedings of the Combustion Institute
www.elsevier.com/locate/proci

Molecular species adsorbed on soot particles issued from low sooting methane and acetylene laminar flames: A laser-based experiment

Y. Bouvier [a], C. Mihesan [a,b], M. Ziskind [b], E. Therssen [a], C. Focsa [b], J.F. Pauwels [a], P. Desgroux [a,*]

[a] *Laboratoire de Physico-Chimie des Processus de Combustion et de l'Atmosphère (PC2A, UMR CNRS 8522), Bâtiment C11, Université des Sciences et Technologies de Lille 59655 Villeneuve d'Ascq cedex, France*
[b] *Laboratoire de Physique des Lasers, Atomes et Molécules (PhLAM, UMR CNRS 8523), Centre d'Etudes et de Recherches Lasers et Applications, Université des Sciences et Technologies de Lille 59655 Villeneuve d'Ascq cedex, France*

Abstract

Recent advances in the field of laser desorption/laser ionization mass spectrometry (LD/LI/MS) have renewed interest in these separation methods for fast analysis of chemical species adsorbed on soot particles. These techniques provide mass-separation of the desorbed phase with high selectivity and sensitivity and require very small soot samples. Combining LD/LI/MS with in situ measurements of soot and gaseous species is very promising for a better understanding of the early stage of soot growth in flames. In this work, three lightly sooting laminar jet flames (a methane diffusion flame and two premixed acetylene flames of equivalence ratio (ϕ) = 2.9 and 3.5) were investigated by combining prompt and 50 ns-delayed laser-induced incandescence (LII) for spatially resolved measurements of soot volume fraction (f_v) and laser-induced fluorescence (LIF) of polycyclic aromatic hydrocarbons (PAH). Soot and PAH calibration is performed by two-colour cavity ring-down spectroscopy (CRDS) at 1064 and 532 nm. Soot particles were sampled in the flames and analysed by LD/LI/Time-of-flight- MS. Soot samples are cooled to −170 °C to avoid adsorbed phase sublimation (under high vacuum in the TOF-MS). Our set-up is novel because of its ability to measure very low concentration of soot and PAH together with the ability to identify a large mass range of PAHs adsorbed on soot, especially volatile two-rings and three-rings PAHs. Studied flames exhibited a peak f_v ranging from 15 ppb (acetylene, $\phi = 2.9$) to 470 ppb (acetylene, $\phi = 3.5$). Different mass spectra were found in the three flames, each exhibiting one predominant PAH mass; 202 amu (4-rings) in methane, 178 amu (3-rings) in acetylene,$\phi = 2.9$ and 128 amu (2-rings) in acetylene, $\phi = 3.5$. These variations with flame condition contrasts with other recent studies and is discussed. The other PAH masses ranged from 102 (C_8H_6) to 424 amu ($C_{34}H_{16}$) and are well predicted by the stabilomer grid of Stein and Farr.

Keywords: Soot; Desorption; PAH; Laser; Laminar flame

* Corresponding author. Fax: +33 3 20 43 69 77.
E-mail address: pascale.desgroux@univ-lille1.fr (P. Desgroux).

1540-7489/$ - see front matter
doi:10.1016/j.proci.2006.08.036

1. Introduction

Soot formation is one of the most challenging problems associated with pollutant formation in combustion processes. Polycyclic aromatic hydrocarbons (PAH) are known to play a key role in the soot inception but the chemical process of PAH and soot formation is not yet fully understood [1]. Another challenge lies in the knowledge of chemical species adsorbed on soot particles because of their potential impact on human health.

Soot, PAH and species adsorbed on soot particle are intimately linked through chemical and physical processes. Soot characterisation includes the soot volume fraction f_v, the optical and morphology properties such as primary particle diameter d_p, aggregate size and particle size distributions. To measure all these properties, several optical and physical sampling methods must be combined. Recent papers show that laser-induced incandescence (LII) for soot concentration and d_p determination [2], scanning mobility particle sizer (SMPS) [3] and small-angle neutron scattering (SANS) [4] techniques for size distribution tend to supplant or complement the extinction/scattering techniques [5]. Concerning PAH detection, species selectivity is generally obtained through probe sampling coupled with gas chromatography (GC) analysis, performed on the gas phase and/or on the condensed species [6], or by molecular beam mass spectrometry [7]. In situ PAH diagnostic can be performed by laser-induced fluorescence (LIF). Although LIF mainly arises from a mixture of PAHs (not a specific one), combined knowledge of both soot and total PAH is important for soot chemistry understanding [8]. Large PAHs react first to form soot precursor particles with a typical size of a few nanometers. While several recent papers have been devoted to nanoparticles identification [4,9,10], only a few studies concern the characterisation of the chemical species adsorbed on soot particles. Hepp and Siegmann [11] established that the photoemission yield from soot particles collected in a methane diffusion flame is enhanced in flame zones containing gaseous PAHs, suggesting the contribution of adsorbed PAHs on soot.

Recent advances in the field of laser desorption/laser ionization mass spectrometry have complemented conventional (and long duration) separation methods for PAH analysis [12]. Fourier transform laser microprobe mass spectrometry (FT-LMMS) was applied in a combustion chamber of an incineration plant [13]. Laser desorption/laser ionization time-of-flight mass-spectrometry (TOF-MS) was applied on Diesel particulate matter collected during driving cycles [14]. Species adsorbed on soot surface have long been considered as being PAH. But a recent study of Oktem et al. [15] in a premixed ethylene flame showed that the early stage of particle growth is dominated by aromatics while the later stage shows a greater contribution of aliphatics. The authors used the photoionization aerosol mass spectrometry (PIAMS) technique [16]. This instrument allows direct sampling and analysis of soot particles in near real time by combining 1064-nm laser desorption and VUV ionization. In previous studies, Dobbins et al. [10,17] identified PAH in the 200- to 472-amu range in an ethylene diffusion flame by LMMS using 266-nm radiation. Aliphatic and light aromatic could not be detected because of their evaporation in the vacuum.

As shown above, selectivity, sensitivity and fast analysis of species adsorbed on soot particles are achievable by laser desorption techniques. However, these techniques remain very difficult to implement and need to be validated through additional measurements. In this work, a new set-up has been designed to study several lightly sooting flames. The experimental strategy combines prompt and temporally delayed LII to provide soot volume fraction and PAH LIF profiles. Calibration is obtained by cavity ring-down spectroscopy (CRDS) allowing very lightly sooting flames to be investigated [18]. The PAH adsorbed on soot are analysed by laser desorption/laser ionization/TOF-MS using a set-up initially designed for doped-ice analysis [19]. In this paper, soot concentration, PAH and chemical species adsorbed on soot are examined in a diffusion methane flame and two premixed C_2H_2 flames having a peak soot volume fraction ranging from 15 to 470 ppb.

2. Experimental

2.1. The burner and the soot collector

The piloted jet burner consists of a hybrid Holthuis burner equipped with a central stainless-steel injector of 4 mm inner diameter. The heat from the lean premixed flat flame of methane serves to stabilize a large range of diffusion or premixed jet flames. Perturbations from ambient air are minimised by an air shroud. Three sooting flames are investigated: a laminar methane diffusion flame ($Q_{fuel} = 0.1\,l\,min^{-1}$) and two premixed C_2H_2/air flames of equivalence ratio (ϕ) 3.5 ($Q_{fuel} = 0.72\,l\,min^{-1}$) and 2.9 ($Q_{fuel} = 0.6\,l\,min^{-1}$).

Soot particles are collected through a collector made of two concentric quartz tubes with holes on the i.d. of the inner tube through which nitrogen is pumped. Fast dilution of samples with nitrogen ensures rapid quenching of chemical reactions. In this study, the collector was placed 50 mm above the burner where it also serves to stabilize the flames. Soot particles are trapped on a porous filter made of borosilicate placed at the top of the collector thus preventing gaseous condensation.

2.2. The LII-CRDS set-up

The laser is a Brilliant Nd:YAG laser operating at 1064 or 532 nm. The LII set-up has been detailed elsewhere [20] and only brief details will be given below. The central part of the unfocussed near-gaussian laser beam is selected using a 1-mm diaphragm and is then directed along x-axis through the flame. The LII distribution along the beam is imaged at right angle onto an ICCD Princeton camera. The gate width of the ICCD camera is 20 ns. It is timed to start at the peak laser pulse (prompt-LII) or 50-ns after the peak (delayed-LII) to discriminate against interference from PAH LIF during 532-nm excitation as detailed below. The detection is broadband. Radiation (532 nm) is rejected with two negative Notch filters. CRDS is a very sensitive line-of-sight technique, which was demonstrated as being very well suited for measuring soot extinction coefficient [18,21]. Using a two-colour approach (532 and 1064 nm), both soot volume fraction and absorption coefficient of the PAH mixture can be obtained. The two-colour CRD set-up used in this work is similar to the one detailed in [18].

2.3. Laser-desorption/photoionisation/time of flight mass spectrometry

The main features of the laser desorption mass spectrometer, previously used to analyse doped-ice samples, have been presented in detail elsewhere [19].

The analyzing technique is based on a 3-step method: laser desorption, UV multi-photon ionization and time-of-flight mass spectrometry. Briefly, the desorption laser (6 ns laser pulse, $\lambda = 532$ nm) is focused at normal incidence on a soot sample area of 1-mm diameter with energy of several milliJoules per pulse. The desorbed neutral molecules are multi-photon ionized by a focused ($\sim$100 μm beam waist) UV ($\lambda = 266$ nm) pulsed laser beam (Continuum ND 6000) with an energy of 50 mJ/pulse. Desorption and ionization lasers are synchronized by a delay/pulse generator (DG 535, Stanford Research System). The produced ions are mass analyzed in a 1-m long Wiley–McLaren TOF/MS equipped with a reflectron (RM Jordan, Inc.). The recording of the transient signals is achieved by a 500 MHz digital oscilloscope (LeCroy 9350 AM) and stored on a microcomputer.

One important challenge associated with the laser desorption/TOF method concerns the soot collection in the flames and the sample stability. It is expected that chemical species identified in the mass spectrometer be representative of those at the sampling location in the flame. Alteration of the adsorbed species might occur (1) during the collection and sample transfer to the spectrometer and (2) during the residence time of the sample in the high-vacuum chamber of the mass spectrometer. The first aspect can be greatly limited using fast thermophoretic sampling [17] or fast nitrogen dilution within a sampling probe [15] to prevent PAHs in the gas phase from adsorbing on the particles. In our work, fast nitrogen dilution has been used as detailed in Section 2.1. The second aspect is linked to the volatility of small PAH under high vacuum. As mentioned by Dobbins et al. [17], LMMS failed to detect aliphatic and light aromatics under 200 amu at ambient temperature. A similar limitation is expected with PIAMS. To prevent evaporation, charge-transfer π-complexing agents can be used [14]. In our work, soot particles, trapped on porous filters, are mounted on a temperature regulated cold finger and cooled to −170 °C to avoid PAH sublimation in the mass spectrometer chamber.

3. Results

3.1. Determination of soot and PAH profiles by using LII

3.1.1. Procedure

3.1.1.1. Two-colour LII vs. prompt-delayed LII. The principle behind two-colour LII [18] is that emission collected from 1064-nm excitation is only assignable to soot while the emission from 532-nm radiation results from both LII signal from soot and LIF from PAH. However, this method requires a careful alignment of the two laser beams and is time consuming. In this work, a variant of the method has been used. In this new method, prompt emission and the 50 ns-delayed emission from 532-nm excitation are collected. While the 50 ns-delayed signal is free from PAH LIF contribution (as confirmed experimentally), the prompt signal might include LIF from PAH in certain regions of the flames. To allow comparison of the two signals, the delayed LII is magnified using a scaling term to account for loss of LII intensity due to soot particle cooling during the delay. This correction factor is calculated at each measurement height of the flame (to account for possible variation of the LII decay rates with height due to variation in soot particle size) using the ratio of measured intensities (i.e. prompt and delayed) at the edges of the flames where PAH is not expected. The difference between the corrected delayed and the prompt signal is the PAH LIF signal. The method is demonstrated in Fig. 1 and compared to the established two-colour LII method. A correction factor of 1.25 was obtained. The very good agreement between prompt (1064 nm) and corrected-delayed profiles indicates that radial variations of soot size, not taken into account by the method, are small using the 50 ns delay. The correction factor with height

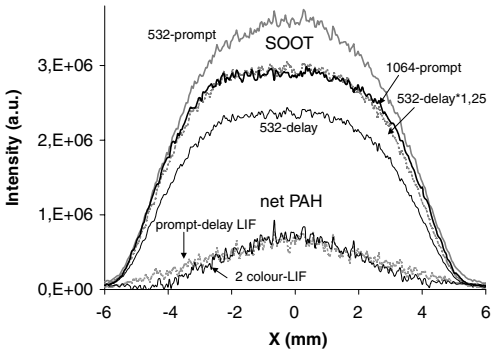

Fig. 1. PAH LIF (bottom part) and soot profiles obtained by prompt-delayed LII at 532 nm or by two colour-LII at 532 and 1064 nm, in methane flame at 35 mm HAB.

of the flames was found to vary within 30% in the methane flame and 10% in the acetylene flames. It is noted that only a selection of PAHs are detected through 532-nm excitation because the spectral range of PAH absorption (and thus fluorescence) shifts towards longer wavelengths as the size of the aromatic structure increases [22].

3.1.1.2. Calibration of soot and PAH. Calibration is based on two-colour CRDS [18]. Line-integrated extinction coefficients (K_{ext}) are measured via 1064-nm extinction measurements while 532-nm extinction results from soot extinction and absorption assigned to the PAH mixture present in the flame.

In a homogeneous medium of length L extinction is related to the soot volume fraction (f_v) by $K_{ext}L = K_e f_v L/\lambda$. The dimensionless soot function $K_e = 4.9$ is obtained using a refractive index value given in [23]. Since jet flames are axisymetric, determination of the local extinction coefficient from the integrated profile is obtained as follows. By translating the burner perpendicularly to the laser beam (i.e. along the y-axis), line-of-sight extinction profiles integrated along x-axis are obtained providing $K_{ext}L(y) = \int_x K_e \lambda^{-1} f_v(x,y)\,dx$. These integrated profiles are compared to integrated-LII profiles obtained for the same burner translation. At each position y of the burner, the radial LII(x,y) profile imaged on the camera is summed along x-axis providing the integrated LII signal: $\mathrm{LII}_{Int}(y) = \int_x \mathrm{LII}(x,y)\,dx$. Figure 2 compares extinction and integrated-LII profiles obtained in the methane flame at 40 mm above the burner (HAB). From the perfect concordance between the profiles, it can be shown that the peak soot volume fraction $f_{vmax}(0,0)$ (250 ppb in this case) can be obtained through:

$$f_{v\,max}(0,0) = \frac{K_{ext}L(0)\lambda}{K_e}\cdot\frac{1}{\int \frac{\mathrm{LII}(x,0)}{\mathrm{LII}_{max}}\,dx} = \frac{K_{ext}L(0)\lambda}{K_e}\cdot\frac{1}{\mathrm{Int}} \quad (1)$$

The value of the normalized integral Int is easily deduced from the radial LII profile at 40-mm HAB. The total absorption coefficient (absorbance) of the PAH is deduced from a similar procedure but using a two-colour approach as in [18]. An example of PAH-absorbance profile at 17 mm HAB is shown in Fig. 2.

3.1.2. Soot volume fraction and PAH absorbance profiles

Radial profiles of PAH and soot volume fraction (f_v) have been obtained at different HAB in the three flames. An example is shown in Fig. 3 at 40 mm HAB.

f_v is found to peak at 256 ppb in the methane diffusion flame. This is consistent with data obtained in a diffusion methane flame stabilised

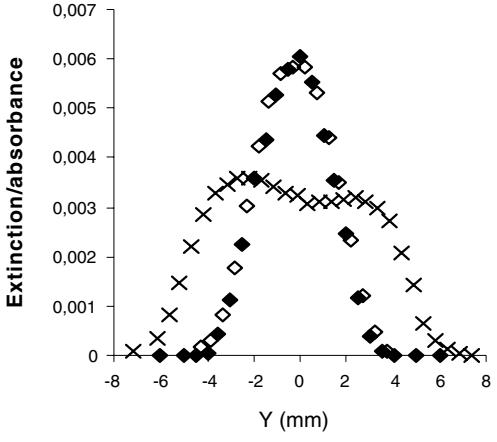

Fig. 2. CRDS (♦) and integrated LII (◊) extinction profiles (1064 nm) in methane flame at 40 mm HAB. PAH-absorbance (532 nm) at 17 mm (×).

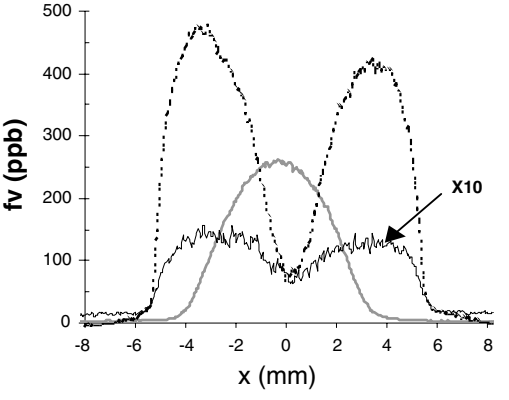

Fig. 3. Radial f_v profiles (calibrated by CRDS) at 1064 and 40 mm HAB. Methane (grey line), acetylene $\phi = 3.5$ (dotted line), acetylene $\phi = 2.9$ (black line, $f_v \times 10$).

on a slot burner [18]. It is 50 times lower than values reported in axisymmetric ethylene diffusion flames [24–26]. Concerning premixed or partially premixed axisymmetric flames, most studies consider ethylene flames with high values of ϕ ($\phi > 5$) [27,28]. Thus, the peak f_v is around 3 ppm ($\phi = 5$) in [28] while f_v peaks at 475 and 15 ppb in our acetylene flames at $\phi = 3.5$ and 2.9, respectively. Clearly, combined use of the sensitive techniques LII/CRDS allows extension of the data base of soot formation towards very lightly sooting flames. This is critical for the understanding of the soot inception process.

The local peak emission intensity at $y = 0$ and the integrated-one (along x-axis) measured on the burner centreline are plotted as function of HAB in Fig. 4. Soot and PAH-LIF signals have been deduced from the prompt/delayed method. In Fig. 4, LII and LIF peak intensities are reported with the same vertical right scale (a.u.) for a given flame. Integrated-LII intensities are converted into integrated extinction coefficients at $\lambda = 1064$ nm using CRDS calibration in each flame. The dimension of the integrated-LIF intensity is arbitrary but directly related to the integrated-LII intensities in Fig. 4. Peak and integrated intensity profiles behave similarly in the methane diffusion flame in which radial profiles of PAH-LIF and soot peak on the burner centreline (Fig. 3). It is not the case in the premixed acetylene flames where annular soot and PAHs profiles present two maxima in the wings along the full height. It is noteworthy that the peak LII signal reaches a maximum while the integrated value continues to grow in premixed flames. By contrast an important decrease of f_v is observed above 40 mm HAB in the methane flame. This behaviour is consistent with the fact that flame heights are quite different: 5 cm (CH_4), 12 cm (C_2H_2, $\phi = 2.9$) and 20 cm (C_2H_2, $\phi = 3.5$). At 45 mm HAB, soot particles of the methane flame undergo oxidation while soot inception and soot growth processes are not yet completed in the acetylene flames.

The methane diffusion flames exhibits two discernible zones assigned successively to PAH and soot as found in a slot burner [18]. By contrast, PAH and soot coexist all along the height of the premixed C_2H_2 flames. At low HAB, the LIF signal is not negligible compared to the LII signal particularly in the methane flame. However at high height, the integrated LIF contribution becomes clearly negligible in comparison with the integrated soot signal. Interpretation in terms of PAH content must be undertaken carefully since LIF profiles only give a picture of part of the PAHs (i.e. high-mass PAHs favoured by visible absorption) present in the flame. PAH absorbance at 532 nm was found to be respectively 3×10^{-3} in the methane flame at 17 mm and 3.5×10^{-3} in the acetylene flame, $\phi = 3.5$ at 40 mm. It was not measurable in the acetylene flame, $\phi = 2.9$.

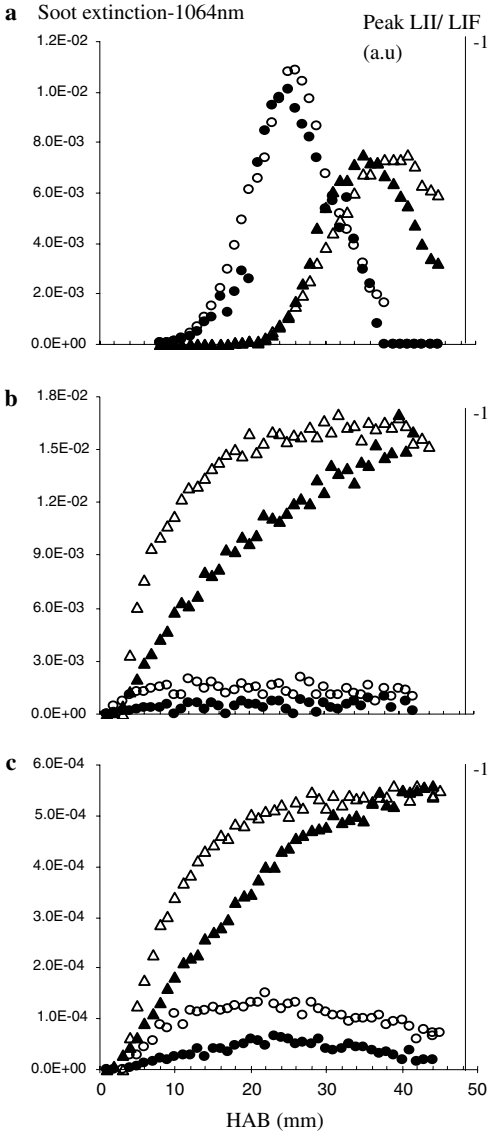

Fig. 4. LII and PAH LIF signals at 532 nm in: (a) methane (b) acetylene $\phi = 3.5$ (c) acetylene $\phi = 2.9$ flames. Peak values (right axis), open symbols; integrated values (left axis), full symbols. PAH, circles; LII, triangles.

3.2. Analysis of the chemical species adsorbed on soot

3.2.1. Preliminary study on pure PAH and "surrogate" soot samples

In order to provide a better understanding of the complex processes involved in laser desorption/multi-photon ionization/TOF-MS analysis method, a 3-step program has been adopted: (1) complete characterization of the laser desorption process on pure or mixed PAH samples; (2) use of "surrogate" soot samples by adsorbing PAHs

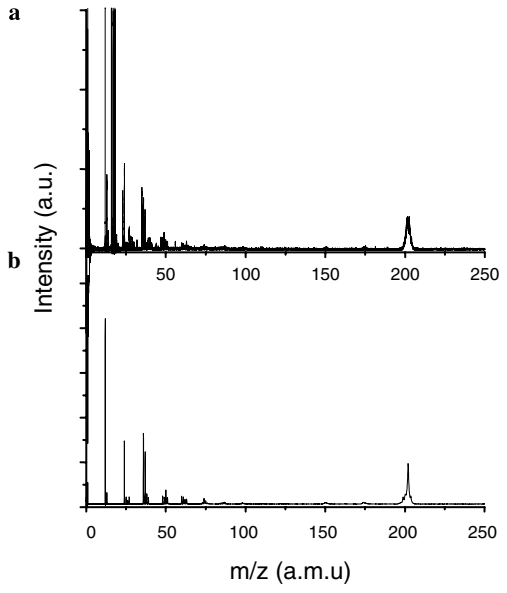

Fig. 5. Laser-desorption mass spectra from (a) charcoal/pyrene mixture, (b) pure pyrene. The samples (2 mm thick tablets) were obtained by pressing 300 mg of pure (>98%) grounded PAH (Sigma–Aldrich)/charcoal mixtures in a hydraulic press.

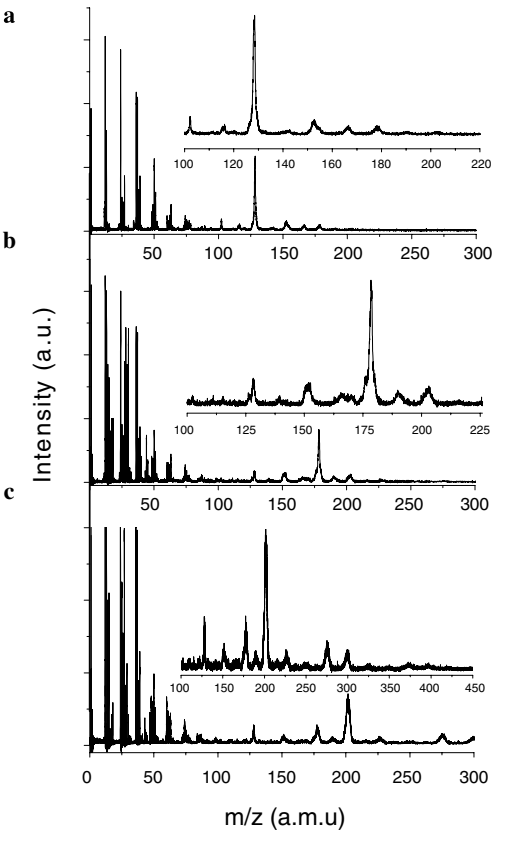

Fig. 6. Laser-desorption mass spectra of the adsorbed phase of soot collected from flames of: (a) acetylene $\phi = 3.5$, (b) acetylene $\phi = 2.9$ and (c) methane. Sampling performed 50 mm HAB.

on graphite or activated charcoal surfaces; (3) analysis of combustion soot samples. The results show a specific response to the desorption laser energy (E_d) for each PAH, defined by a desorption threshold, an optimum laser energy (maximum yield) and a working range. A desorption threshold for carbon around 3.5 mJ/pulse was determined. The working range for PAH desorption is around 2 mJ/pulse, therefore a "smooth" desorption of the adsorbed phase i.e. without affectation of the charcoal matrix nor alteration of the desorbed molecules is achieved.

Mass spectra obtained after laser desorption of pure pyrene and pyrene adsorbed on charcoal are shown in Fig. 5. The mass spectrum of pure pyrene is quite similar to the one obtained by PIAMS [16]. The fragmentation process leads to $C_xH_y^+$ sequences in the low m/z spectrum. This feature does not vary when the PAH is adsorbed on charcoal (or graphite) surface so that observable fragmentation is only assignable to the parent PAH.

3.2.2. Soot sample analysis

Soot samples were analysed by laser desorption just after their collection in flames. Mass spectra are shown in Fig. 6. Each spectrum corresponds to the summation of 10 single-shot spectra. It is noted that spectra from a given position on the soot sample remain quite similar (with continuously decreasing intensities) over tens of laser pulses. Globally, the mass-analyses were found reproducible in terms of mass-identification and main peak intensities.

Although quantitative analysis is not yet achievable, Fig. 6 shows: (1) spectra with a low-m/z part very similar to that one obtained in reference samples (Fig. 5). Therefore, no attempt was made to assign the low m/z peaks to aliphatic molecules fragmentation by contrast to the approach in [15]; (2) mass sequences (high m/z, see expanded spectra in Fig. 6) are observable in each flame sample. Each mass is assignable to a PAH as detailed later; (3) each spectrum is dominated by one PAH.

The mass analysis closely follows the one proposed by Dobbins et al. [10,17] who showed that many of the masses present within soot particles coincide with those (C_xH_y, x and y even) predicted by Stein and Farr [29] to be the most thermodynamically stable (stabilomers). Many PAHs have one or more isomers preventing complete identification to be accomplished. From Fig. 6, we have selected all masses having an intensity of a few % relatively to the main PAH peak of their

Table 1
Masses of PAH stabilomers found in the flames

C	H					
	6	8	10	12	14	16
8	102[1]					
10	126[3]	**128**[1,2,3]				
12		152[1,2]				
14			**178**[1,2,3]			
16			**202**[2,3]			
18			226[3]			
20						
22				276[3]		
24				300[3]		
26				324[3]	326[3]	
28				348[3]	350[3]	
30				372[3]	374[3]	
32				396[3]	398[3]	400[3]
34				420[3]	422[3]	424[3]

[1] C_2H_2, 3.5; [2] C_2H_2, 2.9; [3] CH_4. C and H refer, respectively, to the number of carbon and hydrogen in the stabilomer.
The shaded area represents the stabilomer grid.

corresponding spectrum. Most of them are well predicted by the stabilomer grid [29] as shown in Table 1. The occurrence of the mass increment 24 suggests that growth of the PAH species proceeds through C_2H_2 addition with the release of hydrogen. High-mass PAHs might eventually be fragmented. In addition to those stabilomers, masses 116 (indene), 166, 190 and 318 amu have been detected. Mass numbers (Table 1) strongly depend on the flame, mass sequences shifting towards higher m/z with the following progression: C_2H_2 ($\phi = 3.5$), C_2H_2 ($\phi = 2.9$) and CH_4. Masses vary from 102 to 424 amu, i.e. from one to ten six-membered rings. Comparison with other soot spectra [10,15,17] reveals several major differences: (1) globally our spectra exhibit lighter PAH than those previously reported. PAH with two or three rings are clearly identified. This is likely due to the sample cooling to −170 °C which prevents evaporation of low m/z PAH under vacuum conditions; (2) each flame spectrum exhibits one predominant mass respectively 202 amu in methane flame, 128 amu (naphthalene) in acetylene ($\phi = 3.5$) flame, and 178 amu in acetylene ($\phi = 2.9$) flame. It is likely that 202 amu is pyrene, while 178 amu is anthracene or phenanthrene. That feature contrasts with the idea of the invariance of the soot properties with respect with the composition of the fuel [17].

3.2.3. Discussion

Chemical reaction pathways of PAH and soot formation are beyond the scope of this paper. However some assumptions may be tentatively enounced to explain the spectra characteristics. Remembering that the flame heights (h) are quite different, soot samples were taken at different ratios of (h), specifically 1/4 in acetylene flame ($\phi = 3.5$), 2/5 in acetylene flame ($\phi = 2.9$) and 1/1 in the methane flame; therefore, at different steps of the soot formation process, as confirmed by the soot profiles (Fig. 4). Following this sequence of flames, the most prominent PAH contains two rings (128 amu), three rings (178 amu) and four rings (202 amu), respectively. It should be noticed that Böhm et al. [30] highlighted a new pathway between indene and cyclopentadienyl leading to anthracene and phenanthrene namely two prominent PAHs found on soot sampled in our acetylene flames. This new route in forming PAHs is not included in the H-abstraction C_2H_2 addition (HACA) mechanism [31] and was found particularly important in case of acetylene pyrolysis [30]. Clearly the combined knowledge of the PAH gas phase composition and of the species adsorbed on soot would be extremely useful for understanding the chemical processes involved in soot formation. Although chemical composition is unknown in our flames, some qualitative informations might be obtained from the absorbance measurements at 532 nm. We showed that soot growth process has been completed in the methane flame by contrast to the acetylene flames (see Section 3.1.2) and that soot particles sampled in the methane flame contains heavier PAHs. According to Fig. 4a, PAH LIF intensity greatly increases from 17 mm HAB (where absorbance was measured by CRDS) to its peak at 24 mm HAB. Considering the PAH absorbance values given in Section 3.1.2, it is expected that the methane flame contains much larger concentrations of heavier PAHs than the acetylene flames. In view of establishing eventual correlations between PAH species in the gas phase and those adsorbed on soot, further work will consider PAH absorbance and LIF measurements at different shorter wavelengths to distinguish between classes of PAHs contained in the gas phase.

While the size of the prominent PAHs adsorbed on soot differs in the flames (probably due to the soot maturity at the sampling position), it is difficult to argue now on the influence of the fuel on soot composition. It is believed from our measurements in flames with soot volume fractions ranging from 15 to 470 ppb, that soot concentration is not a sensitive factor affecting the kind of species adsorbed on soot particles.

4. Conclusion

Three lightly sooting laminar jet flames were investigated by combining prompt and delayed LII for spatially resolved measurements of PAH LIF and soot volume fraction. Calibration is performed by CRDS allowing integrated extinction/absorbance through the flames as low as

6×10^{-5} depending on the location. A collector was fixed 5 cm HAB to collect the soot particles for chemical analysis of their adsorbed phase using laser desorption/laser ionization/TOF-MS.

The position of the collector implies that history of sampled soot particles is quite different in the flames extending from 5 cm (methane flame) to 20 cm (C_2H_2 flame, $\phi = 3.5$) and as confirmed by the soot profiles above the burner. Indeed different mass spectra were found in the three flames, each exhibiting one predominant PAH mass; 202 amu (4-rings) in methane flame, 178 amu (3-rings) in acetylene ($\phi = 2.9$) flame and 128 amu (2-rings) in acetylene ($\phi = 3.5$) flame. Other observed PAH masses range from 102 (C_8H_6) to 424 amu ($C_{34}H_{16}$) and are well predicted by the stabilomer grid [29]. It must be emphasized that we have detected lighter PAH, especially 2 and 3 rings PAH, than previously reported [15,17]. This is likely due to the sample cooling to −170 °C. Since the adsorbed phase on soot is linked to the PAH composition within the flame, PAH absorbance at 532 nm has been examined as potential indicator of PAHs. Results are promising and should be completed by additional measurements at shorter wavelengths to detect lighter PAHs.

The specific strengths of our set-up which allows us to detect very low concentration of soot and PAH together with low mass PAHs has been demonstrated. It will be particularly well suited for the study of the early stages of soot formation in flames.

Acknowledgments

The CERLA is supported by the French Research Ministry, by the Nord/Pas de Calais Region and by the European funds for Regional Economic Development. The authors thank the French Research Ministry under the contract D4P3 "Recherche Aéronautique", Jean-Jacques Ledee for technical assistance with the instrumentation, Romain Lemaire for his contribution in soot sampling and Kevin Thomson for fruitful discussions.

References

[1] H. Richter, J.B. Howard, *Prog. Energy Combust. Sci.* 26 (2000) 565–608.
[2] R.J. Santoro, C.R. Shaddix, in: K. Kohse-Höinghaus, J.B. Jeffries (Eds.), *Applied Combustion Diagnostics*, Taylor and Francis, New York, 2002, Chapter 9.
[3] B. Zhao, Z. Yang, Z. Li, M.V. Johnston, H. Wang, *Proc. Combust. Inst.* 30 (2005) 1441–1448.
[4] H. Wang, B. Zhao, B. Wyslouzil, K. Streletzky, *Proc. Combust. Inst.* 29 (2002) 2749–2757.
[5] H. Geitinger, T. Streibel, R. Suntz, H. Bockhorn, *Proc. Combust. Inst.* 27 (1998) 1613–1621.
[6] S. Senkan, M. Castaldi, *Combust. Flame* 107 (1996) 141.
[7] A. Keller, R. Kovacs, K.H. Homann, *Phys. Chem. Chem. Phys.* 2 (2000) 1667.
[8] K.C. Smyth, C.R. Shaddix, D.A. Everest, *Combust. Flame* 111 (1997) 185–207.
[9] P. Minutulo, G. Gambi, A. D'Alessio, *Proc. Combust. Inst.* 27 (1998) 1461–1469.
[10] R.A. Dobbins, R.A. Flechter, W. Lu, *Combust. Flame* 100 (1995) 301–309.
[11] H. Hepp, K. Siegmann, *Combust. Flame* 115 (1998) 275–283.
[12] A. Ciajolo, R. Barbella, A. Tregrossi, L. Bonfanti, *Proc. Combust. Inst.* 27 (1998) 1481–1487.
[13] R. Zimmermann, L. Van Vaeck, M. Davidovic, M. Beckmann, F. Adams, *Environ. Sci. Technol.* 34 (2000) 4780–4788.
[14] V. Carré, L. Vernex-Loset, G. Krier, P. Manuelli, J.F. Müller, *Anal. Chem.* 76 (2004) 3979–3987.
[15] B. Öktem, M.P. Tolocka, B. Zhao, H. Wang, M.V. Johnston, *Combust. Flame* 142 (2005) 364–373.
[16] B. Öktem, M.P. Tolocka, M.V. Johnston, *Anal. Chem.* 76 (2004) 253–261.
[17] R.A. Dobbins, R.A. Flechter, H.C. Chang, *Combust. Flame* 115 (1998) 285–298.
[18] C. Schoemaecker-Moreau, E. Therssen, X. Mercier, J.F. Pauwels, P. Desgroux, *Appl. Phys. B* 78 (2004) 485–492.
[19] C. Focsa, C. Mihesan, M. Ziskind, B. Chazallon, E. Therssen, P. Desgroux, J.L. Destombes, *J. Phys. Conden. Matter* 18 (2006) S1357–S1387.
[20] J. Delhay, Y. Bouvier, E. Therssen, J.D. Black, P. Desgroux, *Appl. Phys. B* 81 (2005) 181–186.
[21] R.L. Vander Wal, *Proc. Combust. Inst.* 27 (1998) 59–67.
[22] A. D'Alessio, A. D'Anna, A. D'Orsi, P. Minutolo, R. Barbella, A. Ciajolo, *Proc. Combust. Inst.* 24 (1992) 973–980.
[23] W.H. Dalzell, A.F. Sarofim, *J. Heat Transfer* 91 (1969) 100.
[24] B. Quay, T.W. Lee, T. Ni, R.J. Santoro, *Combust. Flame* 97 (1994) 384–392.
[25] D.R. Snelling, K.A. Thomson, G.J. Smallwood, Ö.L. Gülder, *Appl. Opt.* 38 (1999) 2478–2485.
[26] M.D. Smooke, R.J. Hall, M.B. Colket, J. Fielding, M.B. Long, C.S. McEnally, L.D. Pfefferle, *Combust. Theory Model.* 8 (2004) 593–606.
[27] A. Mitrovic, T.W. Lee, *Combust. Flame* 115 (1998) 437–442.
[28] C.P. Arana, M. Pontoni, S. Sen, I.K. Puri, *Combust. Flame* 138 (2004) 362–372.
[29] S. Stein, A. Farr, *J. Phys. Chem.* 89 (1985) 3714–3725.
[30] H. Böhm, H. Jander, D. Tanke, *Proc. Combust. Inst.* 27 (1998) 1605–1612.
[31] M. Frenklach, D. Clary, W.C. Gardiner Jr., S.E. Stein, *Proc. Combust. Inst.* 20 (1985) 887–901.

Comments

Phillip R Westmoreland, University of Massachusetts Amherst, USA. You reported unidentified PAH at masses 166 and 190. In a previous work, we sampled toluene and acetylene-fueled flat flames, extracting PAH with

CH_2Cl_2 from collected soot and from an XAD-2 sorbent collecting PAH downstream of the soot filter. Using GC/MS analysis and authenticating standards, we identified the dominant mass 166 species in both flames as fluorene. The dominant mass 190 species was cyclopenta (d,e,f) phenanthrene.

Reply. In our experiments, a few masses, which do not correspond to stabilomers and which do not originate from fragmentation, have been identified in mass spectra. We have not yet attempted to assign those masses to given species. Your comment will be helpful for further assignment.

•

Jonathan H. Frank, *Sandia National Laboratories*, *USA*. The differences in mass spectra that were measured at a single location in three flames were attributed to different soot maturity. This conclusion is based on the assumption that the evolution of soot composition as a function of residence time is the same for these three flames. Do mass spectra acquired at different axial locations within a single flame support this conclusion?

Reply. This is a preliminary study done in very lightly sooting flames. We fully agree that spatially-resolved characterization of the full flame height is needed to confirm our supposition. We are developing a smaller extraction probe to facilitate such a study.

•

Hai Wang, *University of Southern California*, *USA*. Do you have any experimental evidence that the PAHs measured by MALDI are not from adsorption of gas-phase PAHs on soot already deposited on the filter.

Reply. In regions of the flame where gaseous PAHs and soot co-exist, it is likely that PAHs are condensed on the filter during the sampling procedure. In our flames the collector position has been chosen to minimize this effect. In acetylene flames, PAH contribution is thought to be very small according to the very weak fluorescence yield. At the sampling location of the methane flame, soot particles undergo oxidation and PAH fluorescence could not be detected. In this particular case, PAHs detected in mass spectra surely originated from soot particles.

•

Horst-Henning Grotheer, *DLR Stuttgart*, *Germany*. Before species can be absorbed out of soot particles, they have to be formed first. Later on, the absorbed species may be subject to surface reactions. Therefore the question arises whether these species are good messengers to provide evidence on the givens of soot?

Reply. According to the work of Dobbins et al. ([10] in paper) and Öktem et al. ([15] in paper), the analysis of the chemical species adsorbed on soot particles has been shown to help the understanding of the early stage soot mass growth.

The work we have initiated here aims to provide such information in very low sooting flames.

•

Peter Dransfeld, *BASF-AG*, *Germany*. Enthalpies of absorption of high molecular PAH are similar to bond dissociation energies. How can you know that PAH is desorbed only by the LASER desorption process and not synthesized on the surface during irradiation? Is the total amount of desorbed PAH consistent with a surface coverage of less than one?

Reply. In view of testing the entire procedure of soot analysis by LD/LI/MS, we have made an extensive work on mixtures of PAHs and soot surrogates consisting of activated charcoal or graphite on which controlled amount of PAHs were adsorbed. The mass spectra exhibited fragmentation in the low-mass range similar to that seen in Fig. 5. However, absence of PAHs fragments formed from a heavier parent PAH was clearly demonstrated. Furthermore, under the laser fluence conditions we used, the carbon matrix was not affected as indicated in Section 3.2.1. Equally, synthesis of PAH during the irradiation seems unlikely. Concerning the last question, we have not yet made quantitative measurements and are therefore unable to answer.